Brazilian Journal of Medical and Biological Research (2025) 58: e14282, https://doi.org/10.1590/1414-431X2025e14282
ISSN 1414-431X Research Article

Dynactin knockdown leads to synuclein aggregation by blocking autophagy in a zebrafish model of Parkinson's disease

Yongmei Wu[1]*, Qiang Guo[2]*, Jinfan Gan[1]*, Linghan Duan[1]*, Haixia Zhao[1], Haoran Tai[1], Chan Yang[1], Yunzhu Li[1], Zhen Xu[1], Yue Yao[1], Zheng Nie[1], Ming Yang[1], Shurong Li[1], Jun Li[3], and Bingyin Su[1,4]

[1]Development and Regeneration Key Lab of Sichuan Province, Department of Histology and Embryology, Department of Pathology, Chengdu Medical College, Chengdu, China
[2]Department of Basic Medicine, Chongqing Medical and Pharmaceutical College, Chongqing, China
[3]Department of Anesthesiology, Mianyang Central Hospital, Mianyang, China
[4]Chengdu Medical College Infertility Hospital, Chengdu, China

Abstract

Axons of dopaminergic neurons projecting from substantia nigra to striatum are severely affected in the early stage of Parkinson's disease (PD), with axonal degeneration preceding the loss of cell bodies. Our previous study indicated that the dysfunctional retrograde axonal transport could lead to the death of dopaminergic neurons resulting in PD (10.1111/j.1471-4159.2008.05526.x). However, dynein, as the main molecule involved in retrograde axonal transport, was not affected. This study aimed to verify the hypothesis that dynactin rather than dynein may be one of the key factors in the retrograde degeneration of dopaminergic neurons in the early stage of PD. Dynactin morpholino was used to inhibit the expression of dynactin in transgenic (*Vmat2:GFP*) zebrafish, resulting in a significant decrease of diencephalon dopamine neurons and synuclein aggregation in the basal plate region. In the dopaminergic SH-SY5Y cell line, dynactin-siRNA knockdown resulted in the expression of dynein shifting from dispersed distribution to concentration in synapses and cytoplasm near axons, and the fusion rate of dynein to dynactin was decreased, especially in axons, which blocked the retrograde axonal transport of α-synuclein and autophagy flow. Our results linked the knockdown of dynactin gene to the dysfunction of axonal microtubule transport system, suggesting that dynactin may be one of the key factors contributing to the retrograde degeneration of dopaminergic neurons in the early stage of PD.

Key words: Dynactin; Microtubule; Retrograde degeneration; Parkinson's disease; Synuclein; Autophagy

Introduction

The main cause of Parkinson's disease (PD) is the degeneration and death of dopaminergic neurons in the substantia nigra of the midbrain (1). Recent studies suggest that oxidative stress (2), mitochondrial dysfunction (3), abnormal aggregation of α-synuclein caused by the ubiquitin proteasome system (4), and lysosome dysfunction (5) might play important roles in the degeneration and death of dopaminergic neurons. Although many studies have been performed on how to protect dopaminergic neurons from the above factors, the results show that inhibition of the degeneration of dopaminergic neurons could only delay the onset of PD, but not completely prevent its occurrence and development (6–8).

It is generally believed that PD symptoms are not obvious until the loss of dopaminergic neurons is up to 80% in the substantia nigra (9,10), but it is not known what happens before that. Studies indicate that the degeneration of dopaminergic neurons was initially more prominent in the axons and more severe in the substantia nigra striatum system (11). Axons of dopaminergic neurons projecting from the substantia nigra to the striatum were seriously affected in the early stage of PD, and the degeneration of these axons preceded the loss of cell bodies (12). The decrease of synapses projecting to the striatum was more severe than that of neurons in the substantia nigra (9,10). The proportion of synapses lost in

Correspondence: Shurong Li: <lsrsus@163.com> | Jun Li: <lj89199@163.com> | Bingyin Su: <subingyinn@163.com>

*These authors contributed equally to this work.

Received June 16, 2024 | *Accepted January 21, 2025*

the striatum was 50–70% while only 30% in the substantia nigra (13), suggesting that the loss of nerve terminals of dopaminergic neurons in the striatum was more serious than that of neuronal bodies in the substantia nigra. Studies on early PD patients showed that the death of dopaminergic neurons in the substantia nigra of the midbrain not only started from the neuronal bodies, but also from the terminals projecting to the striatum (11). All these studies indicate that the degeneration of dopaminergic (DA) axons in the striatum occurs earlier than that in cell bodies, and axonal degeneration could be an important target for triggering the damage and even the death cascade of dopaminergic neurons in the substantia nigra.

In our previous study, the microtubule depolymerization agent colchicine was injected into the striatum of mice, and the degeneration of the microtubule of DA axon terminals and blockage of retrograde axonal transport were detected, ultimately inducing neuronal death (14), suggesting that the microtubule dysfunction in the axon might play an important role in the pathogenesis of PD. Uchihara proposed that it was the dysfunctional retrograde transport protein that caused the death of dopaminergic neurons and resulted in PD (15). However, the specific mechanism that influences the retrograde axonal transport is unknown. Although dynein is the main molecule involved in retrograde axonal transport (16), our previous study showed that its function was not affected when nocodazole blocked the retrograde axonal transport of striatum-derived glial cell line-derived neurotrophic factor (GDNF) to the substantia nigra, leading to the death of dopaminergic neurons (17). Therefore, this may be due to the dysfunction of some molecule, such as dynactin rather than dynein. On the one hand, dynein always binds to dynactin when it performs its function and hardly acts alone (18). Dynactin can help dynein to bind to RNA, protein, mitochondria, Golgi bodies, and even viral inclusion bodies (19,20).

On the other hand, there is a high correlation between dynactin and PD. In gene analysis of patients with familial PD, it was found that the heterozygous variant dynactin was highly correlated with the occurrence of the disease (21). Knockdown of dynactin reduced the retrograde axonal transport (22). Mutations of dynactin in mice could lead to severe PD symptoms (23). Therefore, we hypothesized that dynactin may be one of the key factors for the retrograde degeneration of dopaminergic neurons in the early stage of PD.

To verify this hypothesis, mycalolide B (MB, a specific dynactin inhibitor) and dynactin morpholino (MO) were used to intervene with the activity and expression of dynactin in Tg (*Vmat2:GFP*) zebrafish, and the changes of dopamine neurons and synuclein aggregation in the diencephalon were observed. Then, dynactin-siRNA knockdown was performed in the SH-SY5Y cell line and the autophagy flow pathway and status of the retrograde axonal transport were investigated.

Material and Methods

Zebrafish strain and maintenance

The AB genetic background zebrafish (*Danio rerio*) were obtained from Southwest University in Chongqing, China, and the Tg (*Vmat2:GFP*) transgenic zebrafish were a gift from Prof. Jiulin Du of the Institute of Neuroscience, China. The zebrafish were raised and maintained at 28.5°C in the zebrafish lab of the Development and Regeneration Key Laboratory of Sichuan Province, where the animal work was conducted. Embryos were staged according to hours post-fertilization (hpf) based on morphological criteria (24). To better observe the internal structures of the embryos, they were incubated with 0.2 mM 1-phenyl-2-thiourea (Sigma, Germany) from 24 hpf to inhibit pigment development.

Zebrafish swimming behavior

Zebrafish larvae at 72 hpf were placed individually into Petri dishes, with a marked coordinate paper placed under the dish. High-resolution cameras were used to record the movement of the zebrafish in the water, and the recordings were analyzed using EthoVision software (Noldus, Netherlands).

Cell culture and treatments

SH-SY5Y cells were obtained from the Cell Bank of the Chinese Academy of Sciences (China) and maintained in a DMEM/F12 nutrient mixture (11320082, Gibco, USA) with L-glutamine supplemented, heat-inactivated FBS (10% v/v), and penicillin–streptomycin (1% v/v) at 37°C under a humidified atmospheric condition containing 5% CO_2. After one week of cultivation, when the cell density reached 80%, cell passage experiments were conducted. In order to obtain a dopaminergic phenotype, the cells were treated with retinoic acid (RA)/phorbol-12-myristate-13-acetate (PMA) in a medium supplemented with RA (10 μM) for three days; then the medium was removed and replaced with growth medium containing PMA (80 nM) for three days. Mycalolide B (60 μg/L) was added to SH-SY5Y cells for 36 h before western blot (WB) and immunofluorescence experiments.

Construction of pCMV-C-BFP-α-Synuclein expression plasmid and stable transfection

α-Synuclein ORF sequence was obtained from NCBI (NCBI; NM_00345.3). The full length human α-synuclein template originated from the recombinant plasmid pDONR221.

SH-SY5Y cells were transfected with pCMV-C-BFP-α-Synuclein using polyethylenimine. 24 h after transfection, the cells were cultured in the pressure selection medium containing 400 μg/mL G418. After 10 ~ 14 days,

the G418-resistant cell colonies were isolated using cloning rings. Cell clones were seeded onto a 6-well plate with 0.5×10^6 cells per well and grown to a density of 100% for 24 h. The cell clone with the highest expression level was subjected to single cell cloning using the limited dilution method. The cell clone was maintained in the culture medium containing 200 μg/mL G418. When the cell density reached 80%, cell passage experiments were conducted. The offspring cells were still cultured in DMEM/F12 nutrient mixture with L-glutamine supplemented, heat-inactivated FBS (10% v/v), penicillin-streptomycin (1% v/v), and 200 μg/mL G418 for subsequent siRNA knockdown experiments.

siRNA knockdown

SH-SY5Y and SH-SY5Y/pCMV-C-BFP-α-Synuclein cells were transfected with dynactin siRNA and negative control siRNA using Oligofectamine and Lipofectamine RNAi Max reagents. Firstly, 0.3 μL dynactin siRNA, 0.75 μL Lipofectamine, and 16 μL opti-MEM were mixed and added to the cells (cells were cultivated in DMEM/F12 nutrient mixture without FBS). After 12 h of cultivation at 37°C, 0.2 μL dynactin siRNA, 0.6 μL Lipofectamine RNAi Max, and 50 μL opti-MEM mixture were added to the cells. After 24 h of cultivation at 37°C, the cells were treated for subsequent experiments.

Transient transfection

Dynactin siRNA was transfected with Oligofectamine and Lipofectamine RNAiMAX reagents, and pCMV-C-BFP-α-Synuclein and mTagRFP-mWasabi-LC3 (donated by Prof. Cuihong Zhou, Peking University, China) were transfected with polyethylenimine. After 24 h of dynactin siRNA transfection using Lipofectamine RNAi Max reagent, pCMV-C-BFP-α-Synuclein plasmid (400 ng), mTagRFP-mWasabi-LC3 plasmid (600 ng), 6 μL polythenimine, and 50 μL Opti-MEM mixture were added to the cells. After 6 h, Opti-MEM culture medium was replaced with DMEM/F12 nutrient mixture with L-glutamine-supplemented, heat-inactivated FBS (10% v/v) and penicillin-streptomycin (1% v/v), and cultivated 24 h for further experiments.

MO and mRNA microinjection

The standard negative control MO and dynactin antisense MO were prepared. Dynactin mRNA was obtained by *in vitro* transcription using a commercial kit (00512434, Invitrogen, USA). All MOs (10 ng/nL) or mRNA (50 ng/μL) were injected into embryos at the 1–4 cell stage to down-regulate or rescue the target genes. Microinjection was performed using a Premium WPI micromanipulator (SYS-PV830, World Precision Instruments, USA).

Protein extraction and western blot analysis

The protein extraction and western blot analysis were performed as described previously (25). The PVDF membranes were probed with primary antibodies overnight at 4°C. After incubation with the horseradish peroxidase-conjugated secondary antibodies for 1 h at room temperature, proteins were detected by chemiluminescence (BIO-RAD,1705061, China). Data acquisition and analysis were performed using ChemiDoc XRS + (BIO-RAD).

TUNEL staining

The SH-SY5Y cells were stained with TUNEL. To evaluate the extent of apoptosis, TUNEL-positive cells in five fields per sample were counted.

Whole mount *in situ* hybridization

Whole mount *in situ* hybridization was performed as described previously (26), using the established antisense probes β-synuclein, th1, and γ-synuclein. The antisense probes were prepared using cDNA (from day 3 embryos) to amplify the template by PCR, and the antisense probe was synthesized according to the kit manual.

Immunofluorescence and image analysis

Immunofluorescence was performed as described previously (25). Primary antibodies were applied at 4°C overnight. Secondary antibodies were added for 1 h at room temperature, then finally washed before being mounted on microscope slides with mounting medium with DAPI. Images were taken with a confocal microscope (Olympus, FV1000, Japan) with the same scanning parameters (HV=500, CV=200) for all samples. Each Immunofluorescence experiment included 12 individuals per group for imaging, and each set of experiments was repeated three times.

Live cell imaging

Cells cultured in a special confocal culture dish were observed using a confocal microscope (Olympus, FV1000) at 24 h after cell processing. Using a 60 × objective lens, the parameters were set to red, blue, and green, and three channels were taken together. One picture was taken every 4 s, with a resolution of 512 × 512, and 40 pictures were taken per cell. Transport of axonal synuclein autophagosome was analyzed by confocal microscopy with acquisition at 0.8 Hz for 120 s. The percentage of moving synuclein autophagosome was evaluated in four different time frames per axon in at least 12 axons per condition.

Statistical analysis

Data visualization and analysis were performed using GraphPad Prism 6 (GraphPad Software Inc., USA). Statistical analysis was conducted using either Student's *t*-test or two-way ANOVA for comparisons between multiple groups, followed by Dunnett's test or Tukey's test for *post hoc* pairwise comparisons. For information on all reagents, please refer to Table 1.

Table 1. All reagents used in the research.

Reagent or Resource	Source	Identifier	Year of purchase
Primary antibodies			
Rabbit monoclonal anti-GAPDH (1:5,000)	Abcam	ab181602	2017
Rabbit monoclonal anti-Lc3 (1:1000)	Cell Signaling Technology	12741	2018
Goat polyclonal anti-Dynactin (1:500)	Abcam	ab11806	2018
Mouse monoclonal anti-p62 (1:500)	Abcam	ab56416	2018
Mouse monoclonal anti-Lc3 (1:500)	Abclonal	A17424	2018
Mouse monoclonal anti-β-tubulin (1:500)	TransGen Biotech	HC101-02	2018
Rabbit anti-synuclein (1:500)	Cell Signaling Technology	4179S	2018
Rabbit polyclonal anti-Dynein (1:500)	Novus	NBP1-90490	2018
Mouse monoclonal anti-tyrosine hydroxylase (1:200)	millipore	AB152	2018
Rabbit anti-Ph3 (1:100)	GeneTex	GTX128116	2018
Secondary antibodies			
Goat anti-rabbit igg Alexa Fluor 488 (1:2000)	Life Technology	A-11008	2018
Goat anti-rabbit igg Alexa Fluor 568 (1:2000)	Life Technology	A-11011	2018
Donkey anti-mouse igg Alexa Fluor 594 (1:2000)	Life Technology	A-21203	2018
Donkey anti-goat igg Alexa Fluor 594 (1:2000)	Life Technology	A-11058	2018
Donkey anti-goat igg Alexa Fluor 488 (1:2000)	Life Technology	A32814TR	2018
Rabbit igg HRP (1:5000)	Abcam	ab6721	2018
Mouse igg HRP (1:5000)	Abcam	ab97046	2018
Goat igg HRP (1:5000)	Millipore	AP003	2018
Chemicals			
L-glutamine	Gibco	Cat. No. 11320033	2019
Fetal bovine serum (FBS)	Gibco	Cat. No. 10099141	2019
Penicillin–streptomycin	Gibco	Cat. No. 15140122	2019
Mycalolide B (MB)	Wako	Cat. No. 13212081	2019
pCMV-C-BFP vector	Beyotime Biotechnology	#D2621	2019
G418	Gibco	Cat. No. 10131027	2019
Polyethylenimine	Polyscience	Cat. No. 24765	2019
Lipofectamine RNAiMAX	Invitrogen	13778075	2019
Oligofectamine	Invitrogen	12252011	
Opti-MEM	Gibco	Cat. No. 11058021	2019
Vitro transcription kit	Invitrogen	Cat. No. 00512434	2019
Antisense probe synthesis kit	Roche	11636090910	2019
TUNEL	Beyotime Biotechnology	C1089	2019
DAPI	Beyotime Biotechnology	Cat. No. P0131	2019
Polyvinylidene fluoride membranes	Millipore	ISEQ00010	2019
Oligonucleotides			
Dynactin siRNA	Life Technology	s98708 and s98707	2019
Negative control siRNA	Life Technology	4390843	2019
Negative control MO	Gene Tools	Customization	2018
5′-CCTCTTACCTCAGTTACAATTTATA-3′			
Dynactin MO (300 μM)	Gene Tools	Customization	2018
5′-GCCGTCTGAACTCATCTTACCGAGC-3′			
Primer: zebrafish TH1 forward	Invitrogen	Customization	2018
5′-cgaattcaagcagctccacatc-3′			
Primer: zebrafish TH1 reverse	Invitrogen	Customization	2018
5′-caatgtctccgatcatcttcc-3′			
Primer: zebrafish β-synuclein forward	Invitrogen	Customization	2018
5′-gaagcacaaggacgaagaagg-3′			
Primer: zebrafish β-synuclein reverse	Invitrogen	Customization	2018
5′-gctggatttgggcttggaatg-3′			
Primer: zebrafish γ-synuclein forward	Invitrogen	Customization	2018
5′-cagcgtccaggatggatgtt-3′			
Primer: zebrafish γ-synuclein reverse	Invitrogen	Customization	2018

Continued on next page

Table 1. Continued

Reagent or Resource	Source	Identifier	Year of purchase
5′-gacaccacagatgtagaggag-3′			
Primer: human α-synuclein forward	Invitrogen	Customization	2018
5'-CGGGAATTCATGGATGTATTCATGAAA-3'			
Primer: human α-synuclein reverse	Invitrogen	Customization	2018
5'-CGGGGATCCGGCTTCAGGTTCGTAGTC-3'			

Results

Knockdown of the dynactin gene led to a decrease of dopaminergic neurons in the diencephalon of zebrafish

The dopamine neurons in the zebrafish diencephalon are similar to those in the substantia nigra pars compacta in humans (27). After knockdown of the dynactin gene through MO or administration of MB, abnormal embryonic development in zebrafish was detected, including spinal deformities and pericardial effusion. The dynactin (DCTN) MO group and the MB group showed increased mortality at 24 hpf, but the mortality rate was significantly lower at 72 hpf. In both the DCTN MO group and the MB group, the swimming distance of 72 hpf zebrafish became shorter and their swimming speed decreased significantly (Supplementary Figure S1).

Tyrosine hydroxylase (TH) antibody was used to label diencephalon dopaminergic neurons at 48 and 72 hpf after the knockdown of dynactin gene through MO. Confocal microscopy showed that the number of TH+ neurons in DCTN MO and MB groups decreased significantly at the above time points (Figure 1A, B, D, E, F, and H). Co-injection of DCTN MO and dynactin mRNA rescued the loss of dopaminergic neurons caused by dynactin MO (Figure 1C, G, M, and N).

In order to verify the effect of dynactin knockdown on the development of diencephalon dopaminergic neurons, TH *in situ* hybridization in 48-hpf embryos was performed, and the decrease of TH expression after dynactin knockdown was detected (Figure 1I and J), which was rescued by dynactin mRNA (Figure 1K). The expression of TH in the MB group was also significantly decreased (Figure 1L), which was consistent with the TH immunohistochemical results. These results suggested that the development of dopaminergic neurons can be affected by the absence of dynactin.

Synuclein aggregation increased in the basal plate region after dynactin knockdown

The accumulation of synuclein is one of the reasons of the degeneration of dopamine neurons. The results showed that although there was no synuclein accumulation in the ventral diencephalon dopaminergic neurons, it was found in the area near the basal plate (the white dotted line indicates the basal plate of zebrafish) in the DCTN MO group and MB group (Figure 2A and B). Because the axons of the dopamine neurons can project to the basal plate area (28), the result implied that axon transportation was blocked after DCTN MO. In order to observe whether the expression of synuclein mRNA was changed, *in situ* hybridization of synuclein was performed. Since there is no α-synuclein in zebrafish, and β-synuclein and γ-synuclein are homologous to human α-synuclein, the latter two were detected in zebrafish. Compared with the control group, no increase of synuclein mRNA was detected in the ventral diencephalon of the DCTN MO and DCTN MO + mRNA groups (Figure 2C). This result indicated that the increase in synuclein aggregation was due to the deficiency of synuclein degradation in the DCTN MO and MB groups.

Dynactin knockdown resulted in synuclein aggregation in SH-SY5Y cells

Because the axons of dopamine neurons project to the basal plate area (28), synuclein may accumulate in the axons if the retrograde transport of synuclein protein in the axons is damaged after the downregulation of dynactin, harming the cells. In order to test this hypothesis, SH-SY5Y cells were used to study the death of dopaminergic neurons *in vitro*. RNA interference was used to knock down dynactin in SH-SY5Y cells. Immunofluorescence and western blot were used to detect the protein level of dynactin in the cells, which was significantly decreased (Figure 3A–C), indicating that dynactin siRNA worked well. Synuclein immunofluorescence staining of SH-SY5Y cells transfected with siRNA showed that synuclein accumulated mainly in axons and in the cytoplasm near axons (Figure 3D and E), suggesting that the down-regulation of dynactin might cause abnormal synuclein aggregation, which was related to axonal transport.

Autophagy pathway was blocked after dynactin knockdown

In order to further explore the cause of synuclein aggregation after dynactin knockdown, the autophagy pathway of synuclein was investigated. Compared with the control group (si-control), the number of autophagosomes in dynactin siRNA group (si-dynactin) was significantly increased and co-labeled with synuclein protein

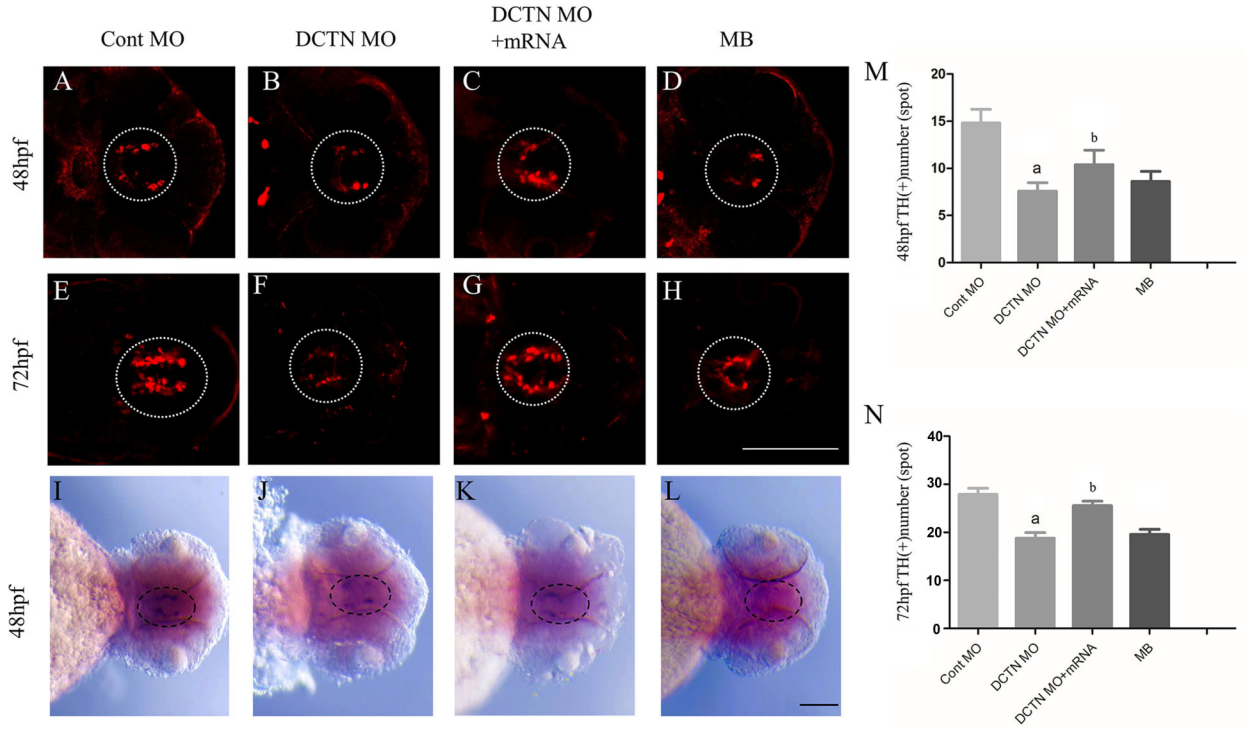

Figure 1. Knockdown of the dynactin gene led to a decrease of dopaminergic neurons in the diencephalon. Immunofluorescence was used to observe the changes of tyrosine hydroxylase (TH)-positive neurons in the diencephalon of zebrafish at 48 and 72 hpf. **A** and **E**, Control MO group; **B** and **F**, DCTN MO group; **C** and **G**, DCTN MO + mRNA group; **D** and **H**, MB group. Scale bar, 100 μm. Expression of TH in the diencephalon of zebrafish was detected at 48 hpf by *in situ* hybridization. **I**, Control MO group; **J**, DCTN MO group; **K**, DCTN MO + mRNA group; **L**, MB group. The white and black dotted lines indicate the ventral area of the zebrafish diencephalon. Scale bar, 200 μm. **M** and **N**, Number of TH-positive neurons in zebrafish diencephalon at 48 and 72 hpf. Data are reported as means ± SD. $^{a}P < 0.0001$, compared with the Cont MO group; $^{b}P < 0.05$, compared with the DCTN MO group (two-way ANOVA, Tukey *post hoc*, n=15–30 zebrafish per group). Cont MO: control morpholino; DCTN MO: dynactin morpholino; DCTN MO + mRNA: dynactin morpholino + dynactin mRNA; MB: mycalolide B.

(Figure 4A and B). There are two reasons for the increase of autophagy: one is autophagy activation, the other is autophagy blocking. In the experiment, mTagRFP-mWasabi-LC3 plasmid was transfected into SH-SY5Y cells to detect the change of autophagy flow. Plasmid mTagRFP-mWasabi-LC3 has red and green fluorescence. If an autophagosome fuses with a lysosome, green fluorescence decreases and red fluorescence increases. If an autophagosome and a lysosome do not fuse, the green fluorescence does not quench and the yellow dots increase (26). The results showed that, compared with si-control, the si-dynactin group formed obvious autophagy and presented increased yellow fluorescent spots (Figure 4C). WB results also showed an increase of p62 and LC3 I and a decrease of LC3 II in the si-dynactin group (Figure 4D and E). Therefore, the abnormal aggregation of synuclein protein in the si-dynactin group was due to the blockage of the autophagy pathway, and the autophagosome formed by synuclein protein could not fuse with lysosomes for metabolism.

Knockdown of dynactin resulted in the inhibition of synuclein autophagosome transport in SH-SY5Y cell axons

The reason why autophagosomes and lysosomes could not fuse was further investigated. A SH-SY5Y/BFP-Synuclein stably transfected cell line was constructed. When dynactin siRNA was transfected into the cell line, synuclein appeared blue (Figure 5A). The transport of autophagosomes formed by synuclein in axons was then observed by transient transformation of mTagRFP-mWasabi-LC3 plasmid in the cell line. The results showed that when dynactin was knocked down, autophagosome transport in axons was blocked, and a large number of autophagosomes accumulated in the axonal colliculus (Figure 5B and E), indicating that the transport of autophagy was affected by the knockdown of dynactin. The above results showed that after knockdown of dynactin, the metabolism of synuclein was affected by the blockage of autophagy flow, resulting in cell death (Figure 5C and F).

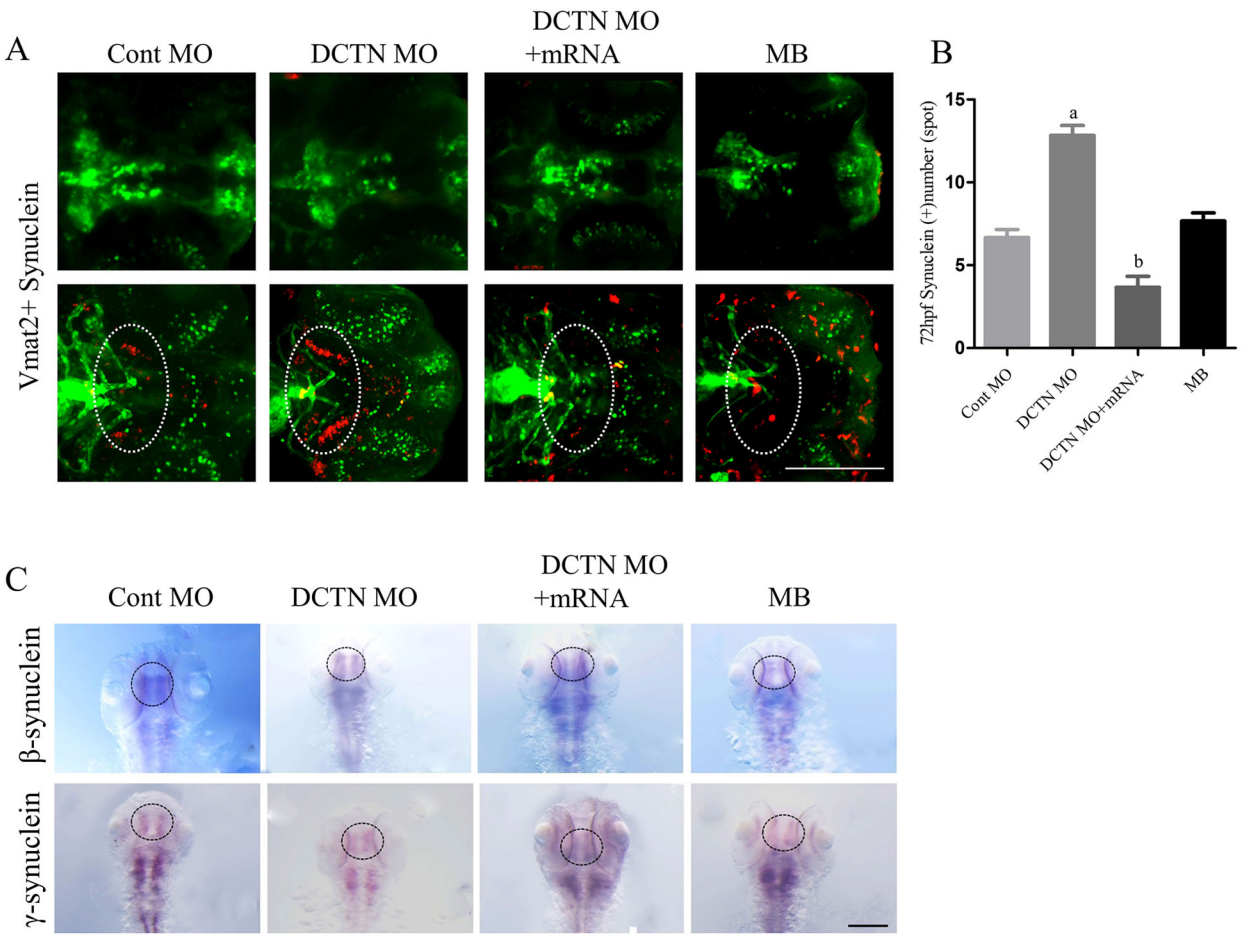

Figure 2. Synuclein aggregation increased in the basal plate region after dynactin knockdown. **A**, Synuclein antibody and *Tg (Vmat2: GFP)* transgenic zebrafish were co-labeled to detect synuclein protein at 72 hpf. The red staining shows synuclein protein, and the green staining shows *Tg (Vmat2:GFP)* transgenic zebrafish. The white dotted line indicates the basal plate of zebrafish. Scale bar, 100 μm. **B**, Number of synuclein-positive spots in zebrafish basal plate region at 72 hpf. **C**, Expression of β-synuclein and γ-synuclein in the ventral diencephalon of zebrafish was detected by *in situ* hybridization. The black dotted line indicates the ventral diencephalon of zebrafish. Scale bar, 200 μm. Data are reported as means ± SD. $^{a}P < 0.0001$, compared with the Cont MO group; $^{b}P < 0.0001$, compared with the DCTN MO group (two-way ANOVA, Tukey *post hoc*, n=15–30 zebrafish per group). Cont MO: control morpholino; DCTN MO: dynactin morpholino; DCTN MO + mRNA: dynactin morpholino + dynactin mRNA; MB: mycalolide B.

It is known that dynactin and dynein form a retrograde transport complex and perform retrograde transport functions (18). Therefore, we knocked down dynactin in the SH-SY5Y cell line and used dynein and dynactin antibodies for co-labeling. The results showed that the expression of dynein in the si-dynactin group shifted from dispersed distribution to concentration in synapses and cytoplasm near axons compared with the si-control group. Dynein was not co-labeled with dynactin in the axon, suggesting that the retrograde axoplasmic transport was blocked (Figure 5D and G). Therefore, the decreased expression of dynactin caused a disorder in synuclein metabolism due to the failure of fusion between autophagosomes and lysosomes as well as retrograde axoplasmic transport obstruction, which may be an important reason for the early onset of PD.

Discussion

Dynactin $p150^{Glued}$ is the largest and most important subunit in the dynactin macromolecular complex. It is involved in the initiation of retrograde axonal transport mediated by dynein and plays an anti-mutation role in stabilizing neuronal microtubules (29). The mutation of DCTN1, which encodes the dynactin subunit $p150^{Glued}$, may lead to various neurodegenerative diseases, including PD (23). In order to investigate how the expression of dynactin in zebrafish affects the process of PD, MB was

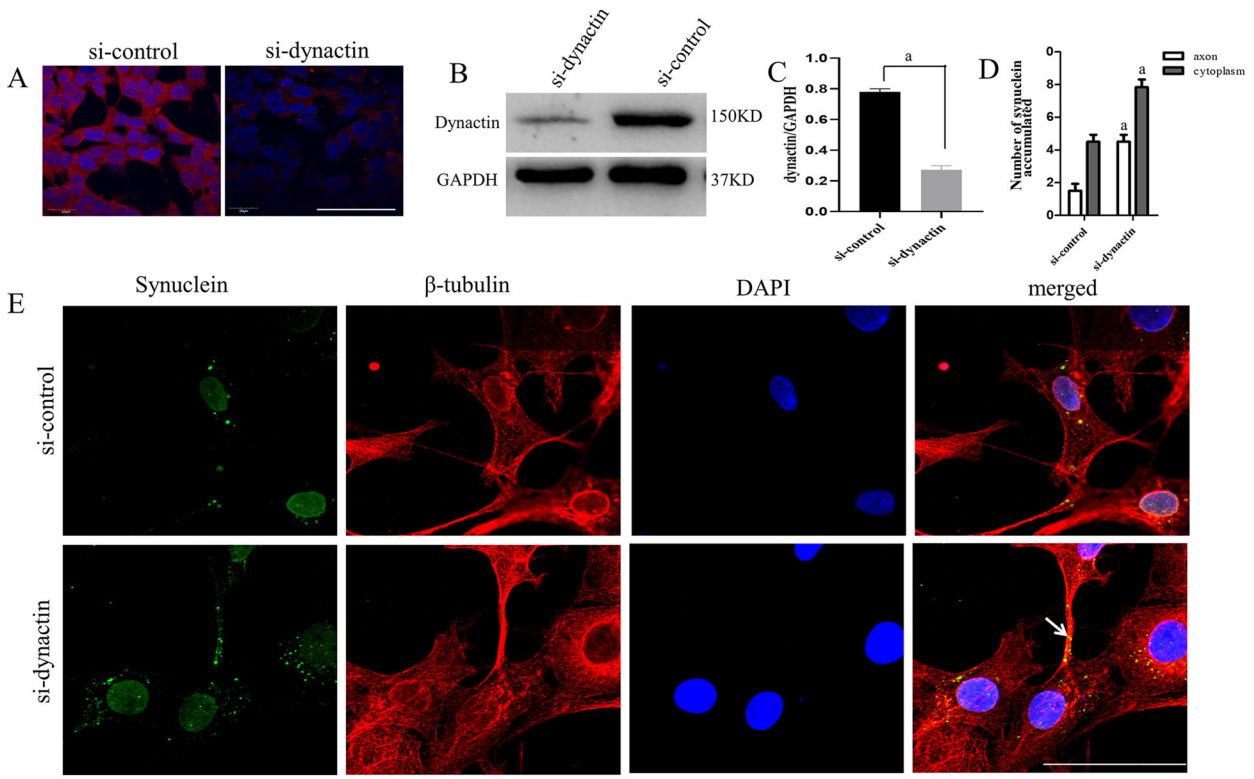

Figure 3. Dynactin knockdown resulted in synuclein aggregation in SH-SY5Y cells. **A**, Expression of dynactin protein in SH-SY5Y cells from the control group (si-control) and the dynactin siRNA group (si-dynactin) was detected by immunofluorescence. The red staining shows the dynactin protein, and the blue staining shows the DAPI stained nuclei. Scale bar, 100 μm. **B**, Expression of dynactin in SH-SY5Y cells was detected by western blotting. **C**, Quantification of dynactin to GAPDH shown in panel **B**. **D**, Number of synuclein accumulated in axons and cytoplasm. **E**, Synuclein and β-tubulin antibodies were co-labeled to detect the expression of synuclein in SH-SY5Y cells from the si-control and si-dynactin groups. The green staining shows the synuclein protein, the red staining shows the β-tubulin protein, and the blue staining shows the DAPI stained nucleus. The arrow indicates the aggregated synuclein protein. Scale bar, 50 μm. Data are reported as means ± SD. $^{a}P < 0.0001$, compared with the si-control group (Student's *t*-test, n=3 biological replicates).

used as a specific inhibitor to dynactin, and Parkinson-like symptoms were subsequently detected. The morphological changes might be related to the mutagenicity and cytotoxicity of MB, and the disequilibrium might be related to neurotoxicity (30). Knockdown of dynactin resulted in increased mortality in zebrafish embryos. Although significantly higher mortality was observed primarily within 24 hpf, malformations were more pronounced at 72 hpf. This suggests that the absence of dynactin severely disrupted organ development in zebrafish, including a smaller head and malformed pericardium. By 72 hpf, the zebrafish nervous system was almost fully developed, indicating that dynactin was involved in abnormal brain development and nervous system dysfunction. In addition, synuclein aggregation was detected in the basal plate region of zebrafish, indicating that the reduced expression of dynactin played a role in the degeneration process of DA neurons, not only altering zebrafish behavior, but also leading to synuclein aggregation. As is well known, the aggregation of α-synuclein in dopaminergic neurons and the formation of Lewy bodies are the most important pathological factors for the diagnosis of PD. Although the use of MPTP in zebrafish could induce a decrease in DA levels and behavioral deficits in model animals, it could not lead to the accumulation of Lewy bodies (31), suggesting that MB might be a better candidate for studying the mechanism of PD.

To further validate the role of dynactin in zebrafish, the effects of DCTN knockdown on embryonic development and dopaminergic neurons in zebrafish were detected. Dynactin affected zebrafish locomotion behavior. After DCTN knockdown, a decrease in dopaminergic neurons in the ventral diencephalon of zebrafish was observed, and further investigation was conducted on the SH-SY5Y cell line.

After dynactin knockdown by RNA interference in the SH-SY5Y cell line, a large accumulation of synuclein was detected in cells, with the distribution mainly concentrated in axons and cytoplasmic axons, indicating that dynactin

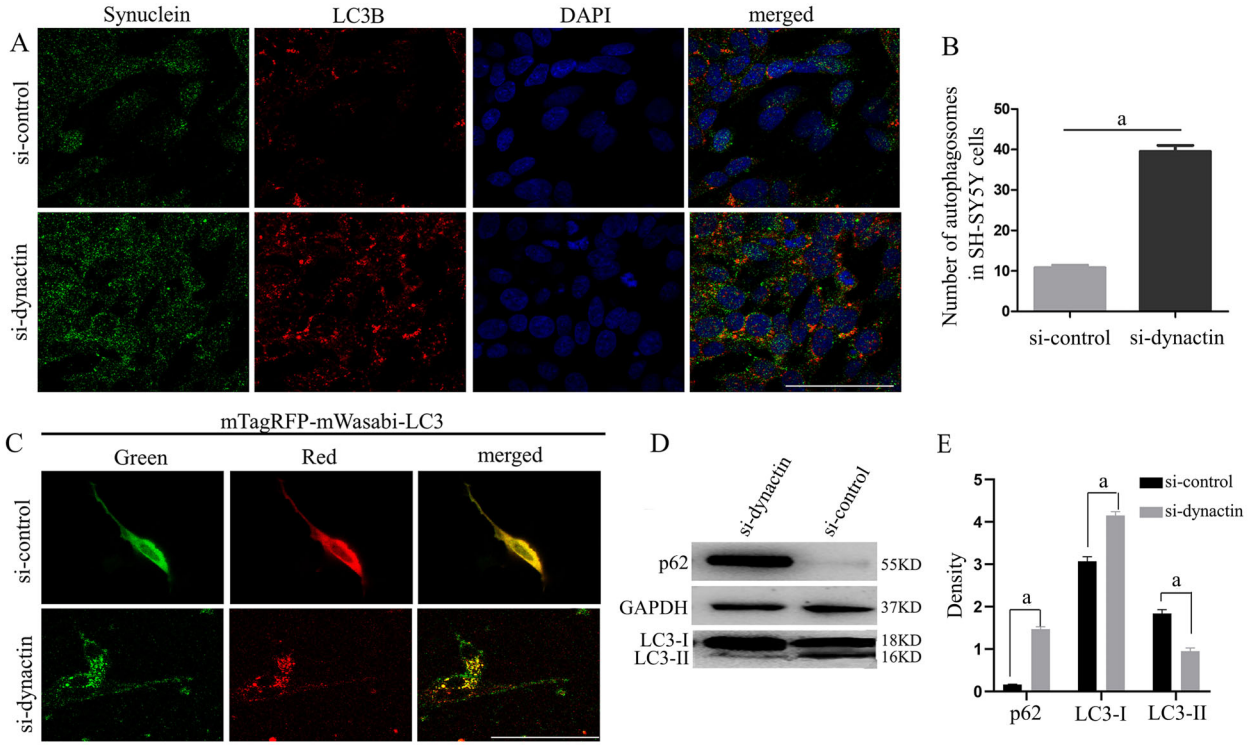

Figure 4. After dynactin knockdown, the autophagosomes formed by synuclein increased abnormally through a blocking pathway. **A**, Co-labeling of synuclein and LC3B proteins in the si-control and si-dynactin groups was detected in SH-SY5Y cells. Green staining represents synuclein protein, red staining represents LC3B protein, and blue staining represents DAPI-stained nuclei. Scale bar, 100 μm. **B**, Number of autophagosomes in SH-SY5Y cells. $^{a}P<0.0001$, compared with the si-control group (t=17.52, df=10). **C**, Autophagy flow in SH-SY5Y cells in the si-control and si-dynactin groups was detected using the mTagRFP-mWasabi-LC3 plasmid. Scale bar, 50 μm. **D**, Expression of LC3 and p62 proteins in SH-SY5Y cells was detected by western blot. **E**, Quantification of p62, LC3-I, and LC3-II relative to GAPDH in panel **D**. Data are reported as means ± SD. $^{a}P<0.0001$, compared with the si-control group (Student's t-test, n=3 biological replicates).

knockdown may lead to the abnormal aggregation of synuclein, which is related to axonal transport. In the process of retrograde axonal transport, a complex is formed between dynactin and dynein to perform the reverse transport function. Previous studies have shown that almost all forms of α-synuclein can be degraded by autophagosomes (32) except α-synuclein of monomer, which is degraded by proteasomes (33). Autophagosomes are formed at the top of axons. Damaged organelles and misfolded proteins are wrapped to form new autophagosomes, which initially move in two directions and then retrograde under the drive of dynein. When they move from the distal axon to the proximal axon, autophagosomes mature and degrade the cargo more effectively (34). In this study, the synuclein accumulation in dopaminergic neurons after knockdown of dynactin in zebrafish was observed. However, it is unclear whether the synuclein aggregation is due to the impaired autophagosome maturation caused by retrograde transport disorder, which in turn affects the clearance of α-synuclein. Therefore, the following study was conducted.

In the living cell workstation, the accumulation of nerve beads resembling axonal transport products was detected in the dynactin knockdown group using the delayed photography technique. To determine whether it was related to the abnormal synuclein aggregation observed in the previous section, the synuclein-BFP and mTagRFP-mWasabi-LC3 plasmids were transfected. In the siRNA knockdown group, synuclein and LC3 showed normal anterograde axoplasmic transport, while retrograde axonal transport was blocked. The changes in intracellular autophagy flow, that is, the accumulation of a large amount of LC3 near the synaptic terminals and around the membrane in the siRNA knockdown group, indicated that the knockdown of dynactin could cause an increase of autophagy at the same locations where the Lewy bodies appeared in dopaminergic neurons in PD patients. Therefore, the decrease of dynactin may hinder the retrograde axonal transport of senescent synuclein, which then accumulate in axons and cytoplasm near the axon end. This distribution is different from the typical site of autophagy increase, which is mainly around the nucleus. The decrease of dynactin leading to changes in

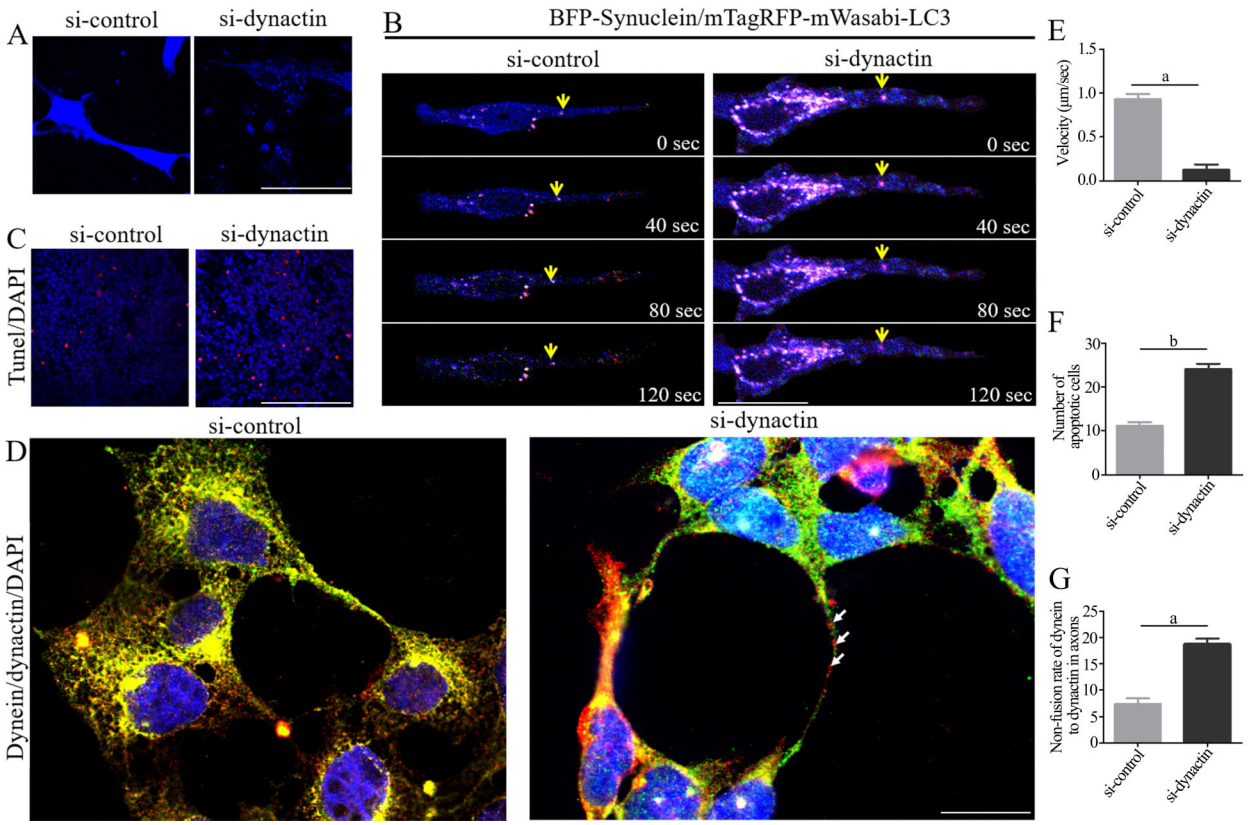

Figure 5. Knockdown of dynactin resulted in the inhibition of synuclein autophagosome transport in SH-SY5Y cell axons. **A**, Expression changes of BFP-Synuclein protein in the si-control and si-dynactin groups. The blue color represents synuclein protein. Scale bar, 50 μm. **B**, The mTagRFP-mWasabi-LC3 plasmid was transiently transfected into SH-SY5Y/pCMV-C-BFP-α-Synuclein cells to detect the transport of synuclein autophagosomes in the axons of the si-control and si-dynactin groups. The blue color represents synuclein protein, and the purple color indicates co-labeling of synuclein and LC3 proteins. Scale bar, 50 μm. **C**, Apoptosis in the si-control and si-dynactin groups was detected by TUNEL assay. The red color represents TUNEL staining, and the blue color represents DAPI staining. Scale bar, 100 μm. **D**, Dynein (red) and dynactin (green) were co-labeled in the si-control and si-dynactin groups. Scale bar, 50 μm. **E**, Average velocities of retrograde synuclein autophagosomes. **F**, Number of apoptotic SH-SY5Y cells. **G**, Non-fusion rate of dynein and dynactin in axons. Arrows: Dynein and dynactin are not co-labeled in the axonal processes. Data are reported as means ± SD. $^{a}P < 0.001$ and $^{b}P < 0.0001$ compared with the si-control group (Student's *t*-test, n=3 biological replicates).

autophagy distribution may be one of the reasons for the final accumulation of synuclein at the above sites.

In summary, after dynactin siRNA knockdown, the fusion rate between dynein and dynactin decreased, especially in axons, which blocked the retrograde axonal transport of synuclein and autophagy flow. This may have a particularly important contribution to the pathogenesis of PD. On the one hand, the pathogenic forms of synuclein could inhibit the stabilizing effect of tau on microtubules, leading to microtubule depolymerization and axonal transport disruption, and ultimately promoting dopaminergic cell loss (35–37). On the other hand, impaired axonal transport was accompanied by impaired autophagosome maturation (38), and autophagy dysfunction was associated with the pathogenesis of PD (39,40). Therefore, dynactin may be one of the key factors contributing to the retrograde degeneration of dopaminergic neurons in the early stage of PD.

Supplementary Material

Click to view [pdf].

Funding

This work was supported by National Natural Science Foundation of China (grant numbers 31801013 and 31600973), Science and Technology Department of Sichuan Province (grant numbers 2019YJ0366, 2021YJ0018, and 2017JY0138), and Development and Regeneration Key Laboratory of Sichuan Province (grant numbers SYS18-01, SYS14-002, and SYS22-05).

References

1. Ben-Shlomo Y, Darweesh S, Llibre-Guerra J, Marras C, San Luciano M, Tanner C. The epidemiology of Parkinson's disease. Lancet. 2024;403(10423):283-292, doi: 10.1016/S0140-6736(23)01419-8.
2. Bej E, Cesare P, Volpe AR, d'Angelo M, Castelli V. Oxidative stress and neurodegeneration: insights and therapeutic strategies for Parkinson's disease. Neurol Int. 2024;16(3):502-517, doi: 10.3390/neurolint16030037.
3. Ebadpour N, Mahmoudi M, Kamal Kheder R, Abavisani M, Baridjavadi Z, Abdollahi N, et al. From mitochondrial dysfunction to neuroinflammation in Parkinson's disease: pathogenesis and mitochondrial therapeutic approaches. Int Immunopharmacol. 2024;142(Pt A):113015. Epub 2024 Sep 1, doi: 10.1016/j.intimp.2024.113015.
4. Zhao Y, Lin M, Zhai F, Chen J, Jin X. Exploring the role of ubiquitin-proteasome system in the pathogenesis of Parkinson's disease. Pharmaceuticals (Basel). 2024;17(6):782, doi: 10.3390/ph17060782.
5. Matsui H, Takahashi R. Current trends in basic research on Parkinson's disease: from mitochondria, lysosome to α-synuclein. J Neural Transm (Vienna). 2024;131(6):663-674, doi: 10.1007/s00702-024-02774-2.
6. Geibl FF, Henrich MT, Xie Z, Zampese E, Ueda J, Tkatch T, et al. α-Synuclein pathology disrupts mitochondrial function in dopaminergic and cholinergic neurons at-risk in Parkinson's disease. Mol Neurodegener. 2024;19(1):69, doi: 10.1186/s13024-024-00756-2.
7. Sechi GP, Sechi MM. Small molecules, α-Synuclein pathology, and the search for effective treatments in Parkinson's disease. Int J Mol Sci. 2024;25(20):11198, doi: 10.3390/ijms252011198.
8. Ko TK, Tan DJY. Is Disrupted mitophagy a central player to Parkinson's disease pathology? Cureus. 2023;15(2):e35458. eCollection 2023 Feb, doi: 10.7759/cureus.35458.
9. Phan JA, Stokholm K, Zareba-Paslawska J, Jakobsen S, Vang K, Gjedde A, et al. Early synaptic dysfunction induced by α-synuclein in a rat model of Parkinson's disease. Sci Rep. 2017;7(1):6363, doi: 10.1038/s41598-017-06724-9.
10. Calabresi P, Mechelli A, Natale G, Volpicelli-Daley L, Lazzaro GD, Ghiglieri V. Alpha-synuclein in Parkinson's disease and other synucleinopathies: from overt neurodegeneration back to early synaptic dysfunction. Cell Death Dis. 2023;14(3):176, doi: 10.1038/s41419-023-05672-9.
11. Caminiti SP, Presotto L, Baroncini D, Garibotto V, Moresco RM, Gianolli L, et al. Axonal damage and loss of connectivity in nigrostriatal and mesolimbic dopamine pathways in early Parkinson's disease. Neuroimage Clin. 2017;14:734-740. eCollection 2017, doi: 10.1016/j.nicl.2017.03.011.
12. Martín-Bastida A, Lao-Kaim NP, Roussakis AA, Searle GE, Xing Y, Gunn RN, et al. Relationship between neuromelanin and dopamine terminals within the Parkinson's nigrostriatal system. Brain. 2019;142(7):2023-2036, doi: 10.1093/brain/awz120.
13. Cheng HC, Ulane CM, Burke RE. Clinical progression in Parkinson disease and the neurobiology of axons. Ann Neurol. 2010;67(6):715-725, doi: 10.1002/ana.21995.
14. Liang Y, Li S, Wen C, Zhang Y, Guo Q, Wang H, et al. Intrastriatal injection of colchicine induces striatonigral degeneration in mice. J Neurochem. 2008;106(4):1815-1827, doi: 10.1111/j.1471-4159.2008.05526.x.
15. Uchihara T. An order in Lewy body disorders: retrograde degeneration in hyperbranching axons as a fundamental structural template accounting for focal/multifocal Lewy body disease. Neuropathology. 2017;37(2):129-149, doi: 10.1111/neup.12348.
16. Yu J, Lai C, Shim H, Xie C, Sun L, Long C, et al. Genetic ablation of dynactin p150Glued in postnatal neurons causes preferential degeneration of spinal motor neurons in aged mice. Mol Neurodegener. 2018;13(1):10, doi: 10.1186/s13024-018-0242-z.
17. Lin S, Liang YJ, Zhang JQ, Bian C, Zhou H, Guo Q, et al. Microglial TIR-domain-containing adapter-inducing interferon-β (TRIF) deficiency promotes retinal ganglion cell survival and axon regeneration via NF-κB. J Neuroinflammation. 2012;9:39, doi: 10.1186/1742-2094-9-39.
18. Verma V, Wadsworth P, Maresca TJ. Human dynein-dynactin is a fast processive motor in living cells. bioRxiv [Preprint]. 2023;29:2023.11.28.569102, doi: 10.1101/2023.11.28.569102.
19. Singh K, Lau CK, Manigrasso G, Gama JB, Gassmann R, Carter AP. Molecular mechanism of dynein-dynactin complex assembly by LIS1. Science. 2024;383(6690):eadk8544, doi: 10.1126/science.adk8544.
20. Gillies JP, Little SR, Hancock WO, DeSantis ME. Cargo adaptor identity controls the mechanism and kinetics of dynein activation. bioRxiv [Preprint]. 2024 Oct 12:2024.10.09.617440, doi: 10.1101/2024.10.09.617440.
21. Aboud O, Parcon PA, Dewall KM, Liu L, Mrak RE, Griffin WST. Aging, Alzheimer's, and APOE genotype influence the expression and neuronal distribution patterns of microtubule motor protein dynactin-P50. Front Cell Neurosci. 2015;9:103, doi: 10.3389/fncel.2015.00103.
22. Lazarus JE, Moughamian AJ, Tokito MK, Holzbaur ELF. Dynactin subunit p150(Glued) is a neuron-specific anti-catastrophe factor. PLoS Bio. 2013;11(7):e1001611, doi: 10.1371/journal.pbio.1001611.
23. Richardson D, McEntagart MM, Isaacs JD. DCTN1-related Parkinson-plus disorder (Perry syndrome). Pract Neurol. 2020;20(4):317-319, doi: 10.1136/practneurol-2020-002505.
24. Kimmel CB, Ballard WW, Kimmel SR, Ullmann B, Schilling TF. Stages of embryonic development of the zebrafish. Dev Dyn. 1995;203(3):253-310, doi: 10.1002/aja.1002030302.
25. Shan M, Lin S, Li S, Du Y, Zhao H, Hong H, et al. TIR-domain-containing adapter-inducing interferon-β (TRIF) is essential for MPTP-induced dopaminergic neuroprotection via microglial cell M1/M2 modulation. Front Cell Neurosci. 2017;11:35, doi: 10.3389/fncel.2017.00035.
26. Huang S, Ma J, Liu X, Zhang Y, Luo L. Retinoic acid signaling sequentially controls visceral and heart laterality in zebrafish. J Biol Chem. 2011;286(32):28533-28543, doi: 10.1074/jbc.M111.244327.
27. Du Y, Guo Q, Shan M, Wu Y, Huang S, Zhao H, et al. Spatial and temporal distribution of dopaminergic neurons during development in zebrafish. Front Neuroanat. 2016;10:115, doi: 10.3389/fnana.2016.00115.
28. Tay TL, Ronneberger O, Ryu S, Nitschke R, Driever W. Comprehensive catecholaminergic projectome analysis

reveals single-neuron integration of zebrafish ascending and descending dopaminergic systems. Nat Commun. 2011;2: 171, doi: 10.1038/ncomms1171.
29. Yu J, Lai C, Shim H, Xie C, Sun L, Long C, et al. Genetic ablation of dynactin p150Glued in postnatal neurons causes preferential degeneration of spinal motor neurons in aged mice. Mol Neurodegener. 2018;13(1):10, doi: 10.1186/s13024-018-0242-z.
30. Chadderton L, Kelleher S, Brow A, Shaw T. Testing the efficacy of rotenone as a piscicide for New Zealand pest fish species. In: Managing Invasive Freshwater Fish in New Zealand, Proceedings of A Workshop Hosted by Department of Conservation, Hamilton, New Zealand; 2001. p113-128.
31. Merghani MM, Ardah MT, Al Shami M, Kitada T, Haque ME. Dose-related biphasic effect of the Parkinson's disease neurotoxin MPTP, on the spread, accumulation, and toxicity of alpha-synuclein. Neurotoxicology. 2021;84:41-52, doi: 10.1016/j.neuro.2021.02.001.
32. Wilfling F, Graef M. Molecular mechanisms and physiological functions of autophagy. J Mol Biol. 2024;436(15):168692, doi: 10.1016/j.jmb.2024.168692.
33. Settembre C, Polito VA, Garcia M. TFEB links autophagy to lysosomal biogenesis. Science. 2011;332(6036):1429-1433, doi: 10.1126/science.1204592.
34. Cason SE, Holzbaur ELF. Axonal transport of autophagosomes is regulated by dynein activators JIP3/JIP4 and ARF/RAB GTPases. J Cell Biol. 2023;222(12):e202301084, doi: 10.1083/jcb.202301084.
35. Jin M, Wang S, Gao X, Zou Z, Hirotsune S, Sun L. Pathological and physiological functional cross-talks of α-synuclein and tau in the central nervous system. Neural Regen Res. 2024;19(4):855-862, doi: 10.4103/1673-5374.382231.
36. Mazzetti S, Calogero AM, Pezzoli G, Cappelletti G. Cross-talk between α-synuclein and the microtubule cytoskeleton in neurodegeneration. Exp Neurol. 2023;359:114251, doi: 10.1016/j.expneurol.2022.114251.
37. Carnwath T, Mohammed R, Tsiang D. The direct and indirect effects of α-synuclein on microtubule stability in the pathogenesis of Parkinson's disease. Neuropsychiatr Dis Treat. 2018;14:1685-1695, doi: 10.2147/NDT.S166322.
38. Boecker CA, Goldsmith J, Dou D, Cajka GG, Holzbaur ELF. Increased LRRK2 kinase activity alters neuronal autophagy by disrupting the axonal transport of autophagosomes. Curr Biol. 2021;31(10):2140-2154, e6, doi: 10.1016/j.cub.2021.02.061.
39. Feng L, Lo H, Zheng J, Weng W, Sun Y, Pan X. Cycloastragenol reduces microglial NLRP3 inflammasome activation in Parkinson's disease models by promoting autophagy and reducing Scrib-driven ROS. Phytomedicine. 2024;135:156210, doi: 10.1016/j.phymed.2024.156210.
40. Liu Y, Qin K, Dou K, Ren J, Hou B, Xie A. TMEM106B knockdown exhibits a neuroprotective effect in Parkinson's disease models via regulating autophagy-lysosome pathway. Biochim Biophys Acta Mol Basis Dis. 2025;1871(1): 167553, doi: 10.1016/j.bbadis.2024.167553.